

Conical Intersections: Relaxation, Dephasing, and Dynamics in a Simple Model

GIL KATZ,^{a,*} RONNIE KOSLOFF,^b AND MARK A. RATNER^a

^aDepartment of Chemistry, Northwestern University, Evanston, Illinois 60208-3113, USA

^bDepartment of Physical Chemistry and Fritz Haber Institute for Molecular Dynamics, Hebrew University of Jerusalem, Jerusalem 91904, Israel

(Received 8 September 2003 and in revised form 26 October 2003)

Abstract. Conical intersections occur on potential energy surfaces of many medium-sized and larger molecules. Their investigation, which has been ongoing for more than six decades, shows that vibronic coupling and relaxation behaviors at conical intersections can become quite complex and show large quantum effects. We present calculations of dynamical behavior in very simple (two-dimensional, degenerate, non-displaced) conical intersection models. The focus is placed on the effects of bath interactions on conical behavior—that is, the extent to which electronic dephasing, nuclear relaxation, and electronic relaxation affect the initially excited wave packet evolving on conical intersection surface. The calculations are carried through using a density matrix picture, with a Lindblad semi-group formalism to characterize relaxation. We observe large quantum effects that act particularly on true conical structures (anti-symmetric with respect to the mixing coordinate), as opposed to comparable-strength interactions without this symmetry. Significant changes in excited-state population decay, and even larger and more striking changes in the (observable) bleach recovery signal, are found.

I. INTRODUCTION

The concept of the potential energy surface serves as the basis for all intuitive understandings, and nearly all instruction, in the areas of molecular structure and dynamics.¹ The Born–Oppenheimer separation² describes completely separable motion, in which electronic states determine potentials for the motion of nuclei. If, however, the Born–Oppenheimer separation held exactly, the world would be much less interesting; there would be no vibronic coupling and therefore metals would have no resistivity, there would be no nonradiative decay,³ and intramolecular electron transfer^{4,5} would behave in a very different fashion.

The simplest way to describe processes by which molecular states evolve from one potential energy surface to another is the Landau–Zener-type crossing,^{6,7} at a point where diabatic surfaces cross and adiabatic surfaces involve an avoided crossing. This is a one-dimensional picture that describes isolated crossings. The Landau–Zener–Stueckelberg view is the basis for most of our understanding, but is a semiclassical analysis for isolated crossings on a one-dimensional configuration coordinate diagram. If the harmonic approximation is combined with the Landau–Zener analysis, the set of

semi-analytic and conceptual results on which much of chemical dynamics and even spectroscopy is based emerges. For example, the Marcus/Hush/Jortner^{4,5,8,9} analysis of nonadiabatic intramolecular electron transfer rates and the important original work of Jortner and his group on nonradiative transitions³ are based on Golden Rule type analyses, which in turn treat the non-adiabatic transitions as weak perturbations.

This entire set of calculations and interpretation is based on the so-called configuration coordinate picture, in which one plots the potential energy (or free energy) as a function of one coordinate of the molecule. Even with the modern understanding that this configuration coordinate should be understood as an energy difference between reactant and product,¹⁰ the description in terms of a single coordinate remains a major oversimplification. The actual dynamics for an N -nuclei system evolves in a space of $3N - 5$ or $3N - 6$ dimensions, depending on whether the molecule is linear or nonlinear. For diatomics, the Landau–Zener approach should be fine, because there is only one degree of freedom that is not either rotational or translational.

*Author to whom correspondence should be addressed. E-mail: gkatz@chem.northwestern.edu

For any larger system, the dynamic evolution is in terms of at least three coordinates, and therefore the condition of near degeneracy of the diabatic potentials reduces it only to a $3N - 6$ or $3N - 7$ dimensional space. The simplest of these situations, beyond the Landau–Zener one-dimensional crossing, is a simple two-dimensional conical intersection. These have been known for more than six decades,¹¹ but their accurate numerical and experimental study has only emerged in the last few years.^{12–28}

In an isolated two-dimensional conical intersection, the two vibrational degrees of freedom correspond to one that actually mixes the two states (analogous to a promoting mode in nonradiative decay theory) and one that accepts the energy as the excited state decays (analogous to an accepting mode in nonradiative decay). The conical intersections result in changes in the state-to-state dynamics, due to the combination of phase evolution and energy flow. They are widespread in reactive systems and can dominate the dynamical evolution. For example, Michl and Bonacic-Koutecky suggested quite early^{16b} that a reaction as fundamental as the cis–trans isomerization of unsaturated hydrocarbons should involve two coordinates, the bond torsion and another. Martinez and coworker have recently^{16c} computed the surfaces, and indeed find that a two-mode conical intersection dominates this photoisomerization.

Models for the simplest two- and three-mode conical intersections at the Hamiltonian level have now been studied quite extensively.^{7,11–31} In the current report, we pursue a less well investigated issue, involving the effect of an external bath on the relaxation and dynamics²⁸ of a conical intersecting system. Early studies of this problem have been reported by a few groups, particularly Domcke and his collaborators,^{29,30,31} who first utilized a Redfield model in which they allowed the vibrational modes that define the potential energy surface of the conical intersection to interact with other vibrational modes, treated as a bath. This is an attempt to deal with anharmonic behavior and vibrational relaxation.

Physically, the effects of the bath mirror the fact that dynamical modes that define the conical intersection are indeed coupled to other modes—including the other modes of the molecule itself, and the modes of a solvent or a colliding system. These external modes can act as energy sinks, and also as dephasing sources. The environmental coupling, then, can cause electronic dephasing, electronic relaxation, vibrational dephasing and vibrational relaxation. Domcke's group, in particular, studied³⁰ the vibrational cooling that occurs by intramolecular vibrational relaxation at conical structures.

Analyses of the relaxation due to external modes and solvents on conical intersection systems, particularly on

pyrazine, have been given by Cederbaum,^{20,24,26} by Robb,²² and by Manthe²⁵ and their collaborators. They used both path integral methods and Redfield analyses, and added linear, bilinear, or quadratic electronic/vibrational couplings. Most recently, Cederbaum and collaborators²⁰ have published benchmark studies on pyrazine and butatriene, in which 24 and 18 modes, respectively, were treated.

The analysis of Domcke's group³⁰ is particularly straightforward. They find a very rapid (10 femtosecond) decay due to active conical modes, and a slower (picosecond scale) relaxation due to vibrational energy relaxation on the lower surface. The simple form taken for the system/bath interaction acts only on vibrations, is bilinear in both the promoting and accepting modes, and ignores pure dephasing as well as electronic relaxation and dephasing. The resulting mechanistic modifications are in fact relatively minor—in particular, they reduce recurrences on the upper conical surface.

An alternative to the Redfield analysis is offered by the semi-group method introduced by Lindblad.³² The advantages of semi-group methods are that they are formally straightforward, they maintain the positive definiteness of the density, and they have a straightforward interpretation in terms of physical behaviors. They are also easy to use, and can include vibrational as well as electronic pure dephasing and relaxation.^{33–39} Here we present an analysis of the simplest conical intersection system, utilizing these semi-group methods. We try to learn how bath interactions affect lifetimes, rates, the evolution of the phase variable around the conical surface, relaxation, and bleach recovery. Using this simplest model, we examine both the flows and the physical behavior in a conical system subject to bath interactions.

II. EQUATION OF MOTION: LINDBLAD APPROACH

We are interested in the behavior of the molecular subunit of the molecule/bath system. We will approach this using the Lindblad semi-group approach,^{32–39} which is easy to use and preserves positivity.

The equation of motion for the density operator $\hat{\rho}$ can be written

$$\frac{\partial \hat{\rho}}{\partial t} = L(\hat{\rho}) = \frac{i}{\hbar} [\hat{H}, \hat{\rho}] + L_D(\hat{\rho}) \quad (1)$$

where the dissipative part will be taken in Lindblad form as

$$L_D(\hat{\rho}) = \hat{F} \hat{\rho} \hat{F}^+ - \frac{1}{2} \{ \hat{F} \hat{F}^+, \hat{\rho} \}_+ \quad (2)$$

with F as an arbitrary Lindblad interaction operator.

The Hamiltonian represents a two-mode and two-electronic surface model. For convenience, we will work in the diabatic picture.^{46–48} Then the two potential energy surfaces can be denoted $|L\rangle$ and $|R\rangle$, having minima to the left and right of the origin (along the x axis). Then

$$\hat{H} = \hat{T} \otimes \hat{I} + \hat{V}_L(x, y) \otimes \hat{P}_L + \hat{V}_R(x, y) \otimes \hat{P}_R + \hat{V}_{LR}(x, y) \otimes \hat{S}_x \quad (3)$$

where

$$\hat{P}_L = |L\rangle\langle L|, \hat{P}_R = |R\rangle\langle R|, \hat{S}_x = |L\rangle\langle R| + |R\rangle\langle L|$$

$$V_R(x, y) = \frac{m\omega_R^2}{2}((x - x_0)^2 + y^2) \quad (4a)$$

$$\hat{V}_L(x, y) = \frac{m\omega_L^2}{2}((x + x_0)^2 + y^2) \quad (4b)$$

$$m\omega_R^2 = m\omega_L^2 = 5 \cdot 10^{-4} \text{ hartrees}$$

Four options for the coupling potential were used:

$$a. V_{LR} = A \tanh(ay) \quad (5)$$

$$b. \hat{V}_{LR} = A |\tanh(ay)| \quad (6)$$

$$c. V_{LR} = A(1 - |\tanh(ay)|) \quad (7)$$

$$d. \hat{V}_{LR} = A \quad (8)$$

where $a = 0.5/\text{\AA}$ and the coupling energy A is varied. We refer to eqs 6–8 as conical, symmetric I, symmetric II, and constant coupling, respectively.⁵⁰

Whether diabatic or adiabatic is the physically more appropriate description will depend^{46,47,49} both on the mixing term V and on the relaxation described by the last term in eq 2. As A increases, the adiabatic picture best describes physical behavior. Far from the crossing point, either description is appropriate, so we will use both.

Both electronic and vibrational dissipative operators can be used.^{36, 38, 41, 44, 45}

$$\hat{F}_v = \sqrt{k_\downarrow} \hat{a} \quad (9)$$

$$\hat{F}_e = C_e \otimes \begin{pmatrix} 0 & 1 \\ 0 & 0 \end{pmatrix} \quad (10)$$

$$\hat{F}_d = C_d \otimes \begin{pmatrix} 1 & 0 \\ 0 & -1 \end{pmatrix} \quad (11)$$

where:

$$C_d = \frac{1}{\sqrt{T_2}}$$

and $1/T_2$ varies from 10^{-3} to 10^{-6} hartrees. The operator \hat{a} destroys a vibrational quantum in the x coordinate, and $k_\downarrow = 10^{-8}$ hartrees. The initial wave packet state before excitation was chosen as: $\hat{\rho}(0) = |\psi_{00}\rangle\langle\psi_{00}| \otimes \hat{P}_R$, where ψ_{00} is the ground vibrational state on the $|R\rangle$ electronic surface.

By choosing F to permit vibrational relaxation (eq 9), electronic relaxation (eq 10), and pure electronic dephasing (eq 11), we can examine a range of bath effects on the dynamics and relaxation on both conical (eq 5) and related (eqs 6–8) potential surfaces. The temperature of the bath was assumed to be zero.

The calculations were completed by direct Newton propagation of the density matrix in time, using grid methods discussed in refs 40 and 41. Because the bath permits vibrational relaxation and electronic dephasing, we can extend earlier work on vibrational and electronic bath interactions on conical intersection dynamics, and compute both characterizing behavior (short time dynamics) and important experimental observations (bleach recovery).

The potential surfaces corresponding to the conical intersection that we choose to study are given in Figs. 1–3. Figure 1 shows the adiabatic representation of the potential energy surface—notice the symmetry of this simple two-dimensional conical as described by eq 4. Figure 2 shows the diabatic representation, in which there is a seam corresponding to degeneracy of the left and right potentials at precisely the value $x = 0$. The potentials will cross at this seam, but their relative slopes will differ depending on the position along the seam.

In the adiabatic potential of Fig. 1, the crossings are avoided. A more close-up view of this picture is shown in Fig. 3: following photoexcitation from the ground state, the wave packet will evolve on the excited state, undergoing rapid and effective transition to the ground state only near the avoided crossing (shown at the origin in Fig. 3).

Conical intersections have been invoked to explain the very rapid decay from the excited to the ground state. In most physical situations, of course, the curves are not so symmetric as they are in Figs. 1–3: usually, there is either warping of the ground-state surface or a breaking of the symmetry by some chemical substitution, so that the conical intersection does not occur at the center of symmetry of the systems. Investigation of inequivalent minima, along with specific investigations of coherence conservation and with effects of distorting the potential energy surface away from the very symmetric case of Fig. 3 will be pursued in subsequent research.

The problem that we will study here involves relaxation after photoexcitation: the initial state of the system

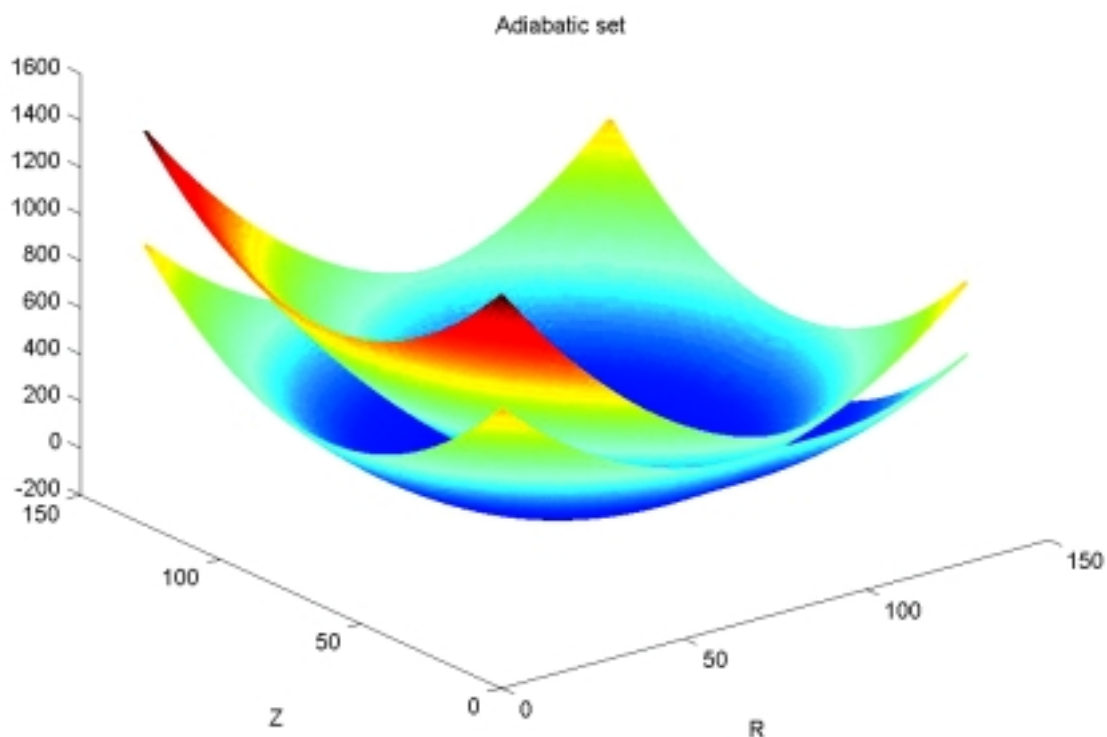


Fig. 1. An adiabatic representation of the two electronic potential surfaces. Distances in Å. Parameters are: $m\omega_R^2 = m\omega_L^2 = 5 \cdot 10^{-4}$, $a = 0.5/\text{Å}$, $A = 0.2 \text{ eV}$, $x_0 = 0.5$.

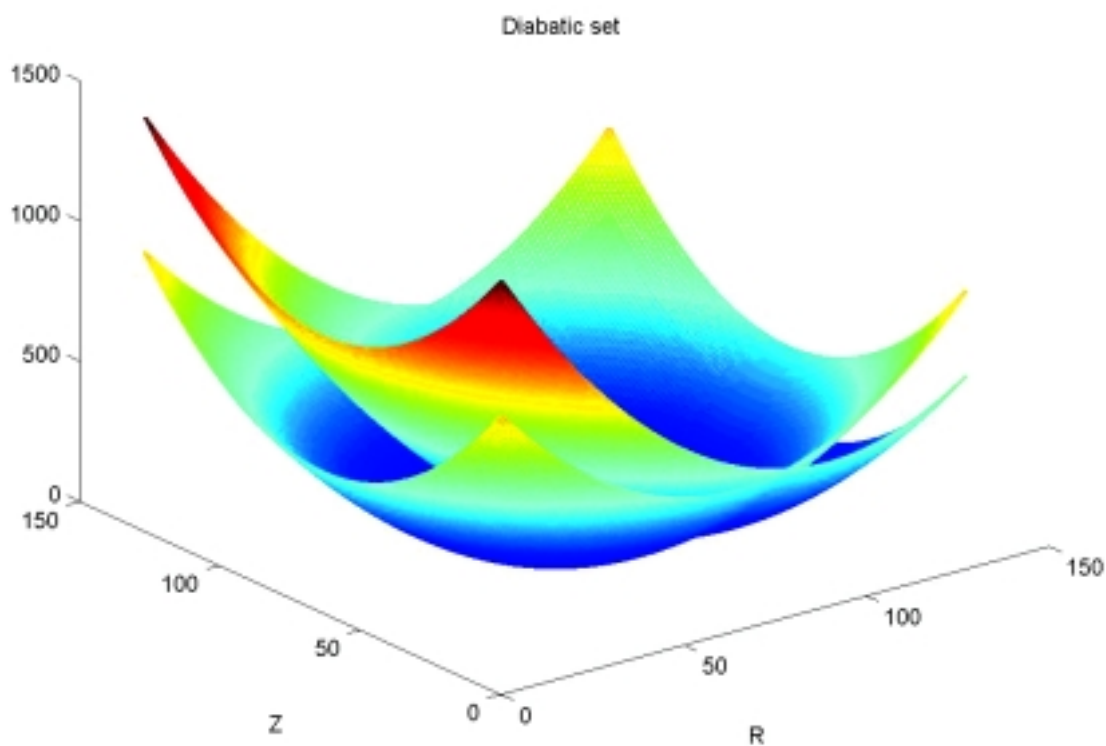


Fig. 2. A diabatic representation of the two electronic surfaces.

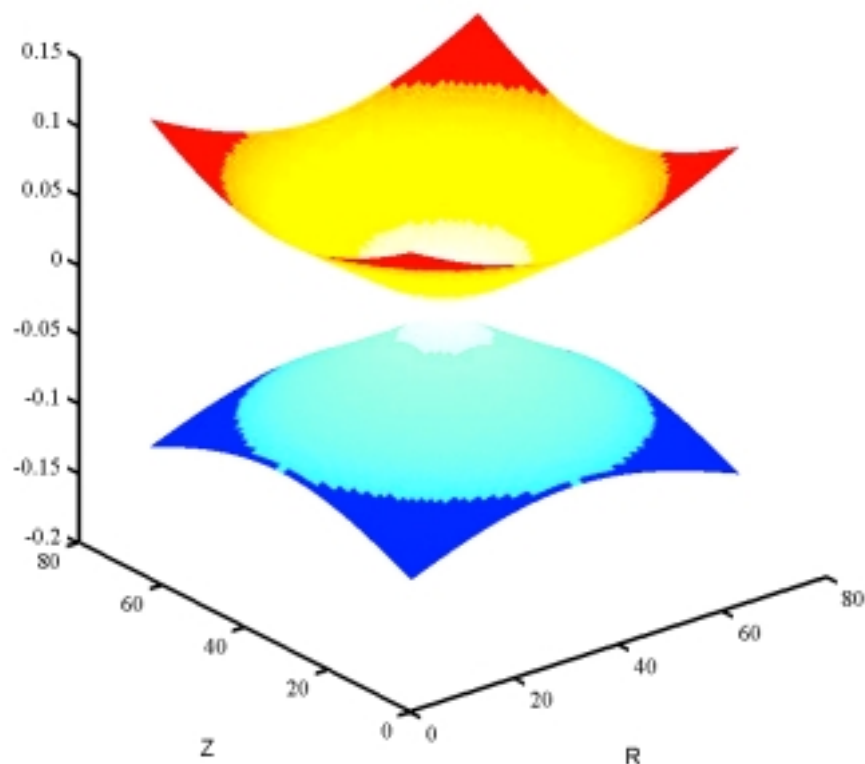


Fig. 3. A close view of conical intersection within the adiabatic representation.

is taken to be in one of the minima on the diabatic surface, and then photoexcited assuming a very fast laser, to form a Gaussian packet on the excited state. It is the dynamics of this excited-state Gaussian wave packet that we wish to pursue.

The newly created wave packet on the excited state will begin to move on the isoenergetic contour, which corresponds to the upper part of a cone, as indicated in Fig. 3. At the same time, dephasing effects will reduce the fidelity of that rotation to classical predictions, and vibrational relaxation will bring the excited state down towards the minimum at the origin.

In the relaxation process we expect some competition between the mixing terms of eqs 5 to 8, which will cause the packet excitation to transform to the other diabatic minimum, and the vibrational relaxation term of eq 9, which will cause the excited packet to move quickly down towards the crossing.

Experimentally, the bleach recovery consists of measuring the expectation value of the projector onto the initial state, given by $\hat{\rho}(0)$.

In the simple Landau–Zener picture, one expects to see turnovers (that is, non-monotonic behavior of the relaxation rate or the bleach recovery), as the parameters either of the Hamiltonian or of the bath mixing are varied. One of the major aims of the current research is

to see how well this expectation is met in the case of conical intersection behavior.

III. RESULTS

Our aim here is to examine the dominant behaviors in the symmetric, two-mode conical intersection of Figs. 1–3. We focus on two physical behaviors, the population on the excited state and the recovery of the bleach (recovery of the population of the ground vibrational state in the initial diabatic minimum). The behavior will be examined as a function of the form (eqs 5–8) and the magnitude (A parameter) of the vibronic coupling. The other variables of interest are the strength of the electronic dephasing term of eq 11 given either by C_d or by its square, the inverse of the transverse relaxation time. Finally, we will be interested in slightly different state preparations: in every case, the excited state will be taken as a Franck–Condon wave packet. In some instances, though, the wave packet will be given a component of initial momentum around the upper cone surface (in the y coordinate). When the nuclear dephasing terms (not treated here) are strong, we expect this rotatory motion to eventually slow down, so that there will be no more effective centrifugal barrier forcing the rotation to occur away from the minimum. For a small amount of initial angular momentum around the cone, the system

explores two-dimensional space, whereas if the rotation is effectively quenched by relaxation processes, the simplest cartoon version of the two-dimensional potential now becomes the one-dimensional, Landau–Zener potential. The Hamiltonian parameters given under eqs 4 and 8 will be retained throughout.

Figure 4 shows the effects of changing electronic dephasing and the form of the mixing term on the $|L\rangle$ state (adiabatic) population. For the conical mixing of eq 5, as well as the symmetrized form of eq 6 and the constant mixing of eq 8, the $|L\rangle \rightarrow |R\rangle$ transition rate increases monotonically with increased dephasing strength. The pronounced multiple oscillations found with the constant mixing are much reduced either with the conical form of eq 5 or with its absolute value. Indeed, as the dephasing strength increases, the population evolutions resulting from eqs 5 and 6 become identical (Fig. 5), and the oscillations vanish, since the excited state becomes largely depopulated by 400 fs, for $1/T_2 = 0.0004$.

Within the relatively small range that we explored ($0.05 \text{ eV} < A < 0.2 \text{ eV}$), the rates of population decay increased monotonically with increasing A for all four mixing forms. Both on general terms⁴² and based more specifically on results found for simple avoided crossings,^{38,39} one expects turnaround behavior (with decay decreasing upon either increasing or decreasing A values

away from some value A_{MAX}). Apparently, $A_{\text{MAX}} > 0.2 \text{ eV}$ for this system. The relatively close approach of the two left-most curves in Fig. 6 suggest that A_{MAX} should be slightly above 0.2 eV .

One experimental way to characterize conical intersection dynamics is to measure the repopulation of the ground state following an excitation bleach. Conceptually, wave packets are excited to the upper state surface, cross near the conical apex, and relax (vibrationally) on the ground state to repopulate P_{00} . This suggests that the bleach recovery rate would, in the simplest case, increase monotonically with A , with $1/T_2$ and with $1/T_1$ (for all of these parameters small enough to avoid turnovers).

Figure 7 shows the predicted bleach recovery for our standard parameter values. Several striking behaviors are seen. First, the recovery starts smoothly from zero, just as it should. The behavior, however, is not monotonic in time—the population of P_{00} eventually starts to drop again, at least for the symmetric mixing terms of eqs 6 and 7. This is most simply thought of in terms of localization: for packets moving on the lower surface with small enough $1/T_1$, the expansion in terms of vibrational harmonic eigenstates will exhibit oscillations whose approximate frequency will be that of the fundamental harmonic vibration—a similar explanation (with a higher effective frequency) can explain the oscillating behavior in Fig. 4, for small $1/T_2$.

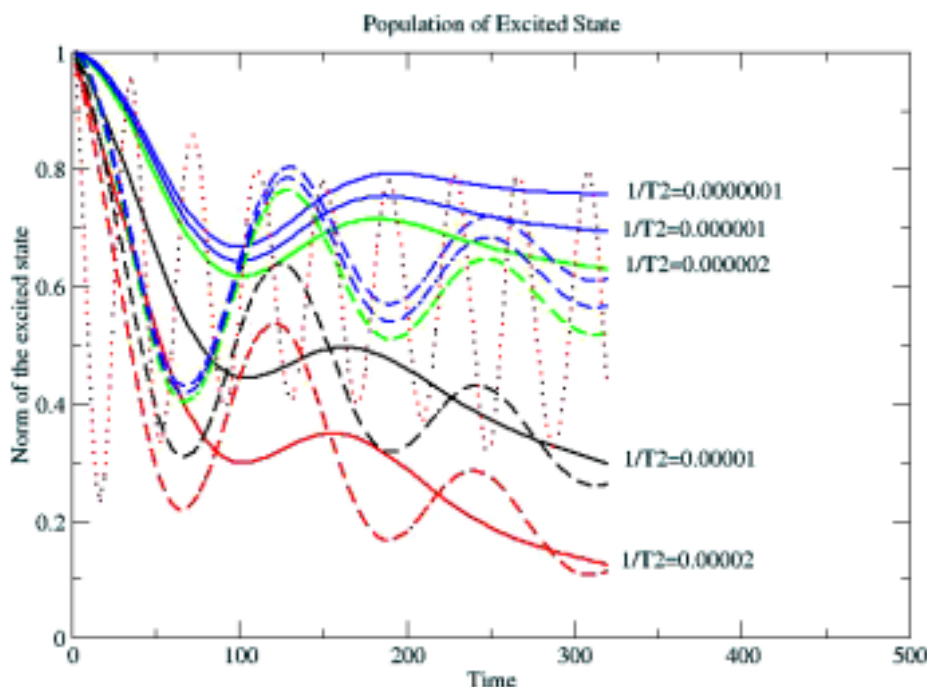


Fig. 4. The $|L\rangle$ state (adiabatic) population as a function of time for different values of $1/T_2$ displayed for the conical intersection (solid line), the symmetric I coupling (dashed line) and constant coupling (dotted line). Parameter values: $k_{\downarrow} = 10^{-8}$ hartrees, $1/T_1 = 10^{-8}$ hartrees.

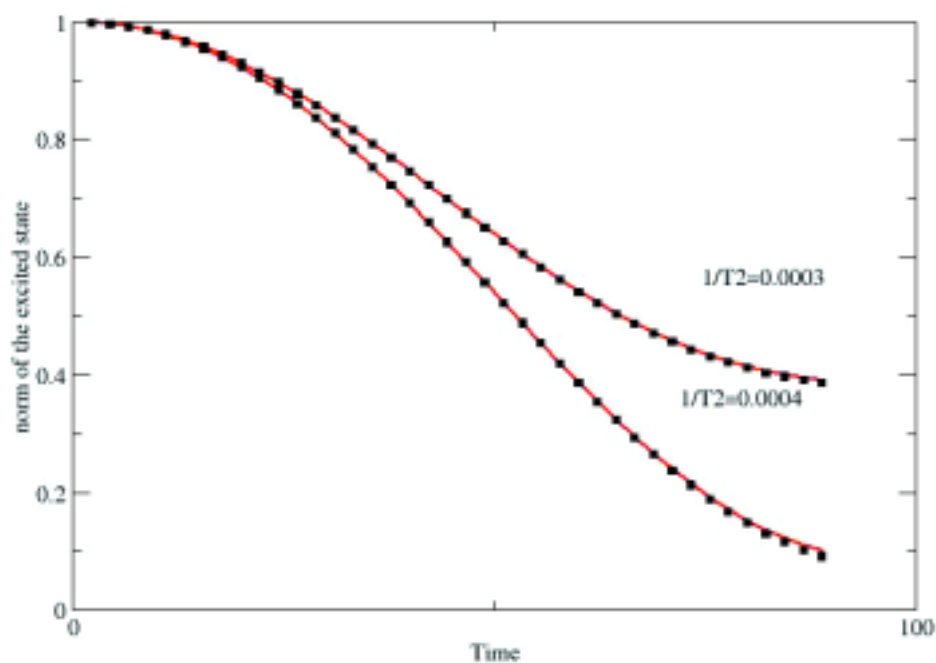


Fig. 5a. Population of $|L\rangle$ state as a function of the time for large $1/T_2$. Results shown for the conical intersection (solid red line) and the symmetric I coupling (dotted black line). The figure shows that for strong electronic dephasing the asymmetric and the symmetric coupling parameters as in Fig. 4 give similar behavior.

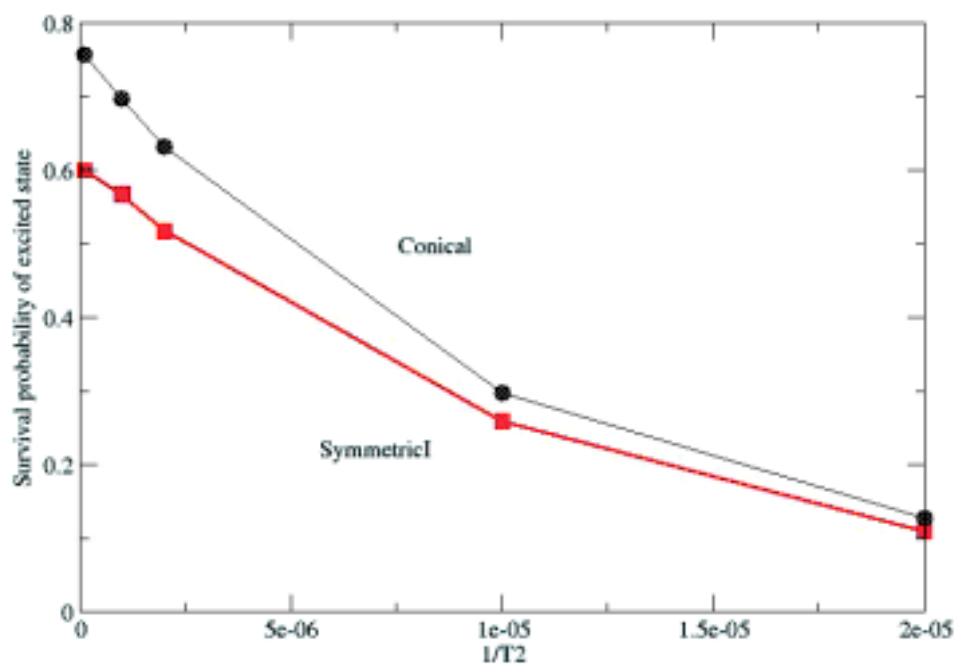


Fig. 5b. The survival probability of the $|L\rangle$ state as a function of $1/T_2$. It is clear that at small $1/T_2$ survival probability is higher for the conical system and as $1/T_2$ grows, the asymmetric and the symmetric I systems coincide.

As the electronic dephasing becomes stronger, the bleach recovery is faster. This probably reflects the increased population on the lower adiabatic surface, as seen in Fig. 4.

A striking result of Fig. 7 is that for the conical potential of eq 5, the bleach recovery is extremely slow for weak electronic dephasing. This is unexpected since the relative decay rates of Fig. 5 become the same for

eqs 5 and 6 when $1/T_2$ is large enough and are similar in magnitude, even for small $1/T_2$. Another result (Fig. 8) is that the bleach recovery also vanishes if the momentum in the y coordinate of the initially excited wave packet vanishes, that is, if the initial wave packet on the excited state is given no initial momentum in the y direction. Figure 8 also shows that the bleach recovery with the symmetric I potential of eq 6 is essentially insensitive to

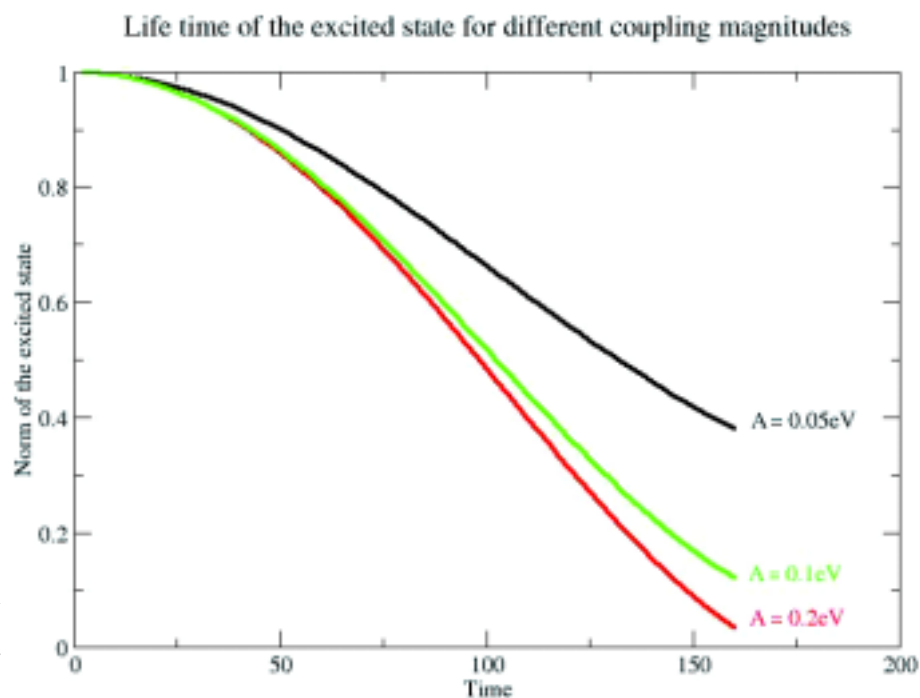


Fig. 6. Evolution of population on the $|L\rangle$ state for different magnitudes of the coupling in the conical system. Parameter value $1/T_2 = 3 \cdot 10^{-5}$ hartrees.

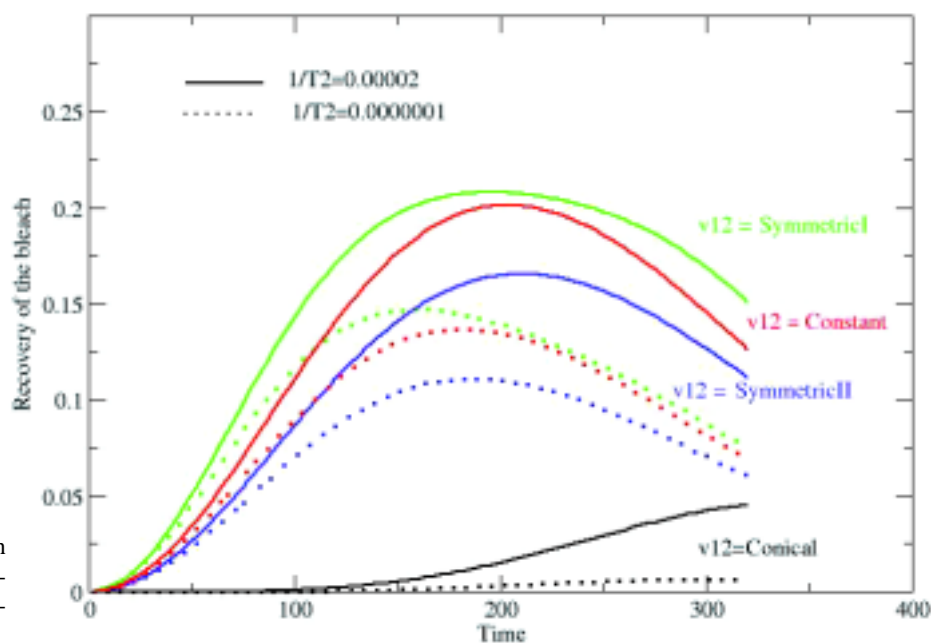


Fig. 7. Recovery of the bleach as a function of time for different coupling forms at two different values of $1/T_2$.

initial y momentum, while the conical interaction (eq 5) actually gives a turnover behavior in the y momentum dependence.

The fact that the bleach recovery vanishes for zero y momentum, and essentially vanishes for sufficiently small $1/T_2$, while the symmetric mixing terms and the constant mixing do not show such behavior must reflect the fundamental symmetry differences.^{7,11,22,43}

The causal part of the quantum Liouville eq 1 shows that the rate of change of the populations $\dot{\rho}_{ii}$ is proportional to i times the coherences, while $\dot{\rho}_{ij}$ is proportional to $i(\rho_{ii} - \rho_{jj})$.

Figure 9a thus shows the four density elements $\rho_{LL}(x,y)$ (upper left), $\rho_{LR}(x,y)$ (lower left), $\rho_{RL}(x,y)$ (lower right), and $\rho_{RR}(x,y)$ (upper right), projected on the adiabatic potentials. Figure 9a is plotted instantaneously

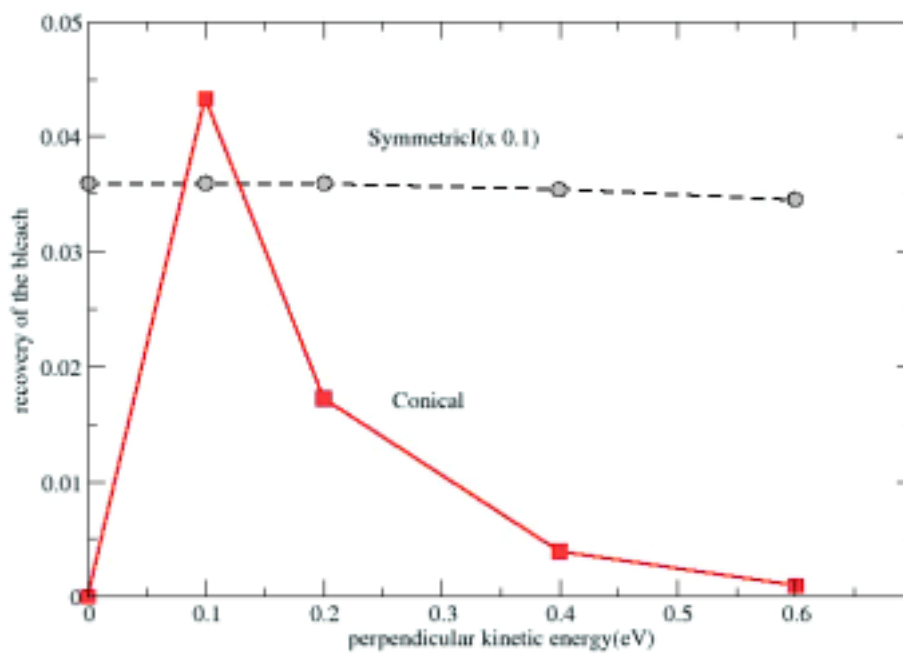


Fig. 8. Recovery of the bleach at 150 fs as a function of initial kinetic energy perpendicular to the curve crossing, for two functional forms of the coupling.

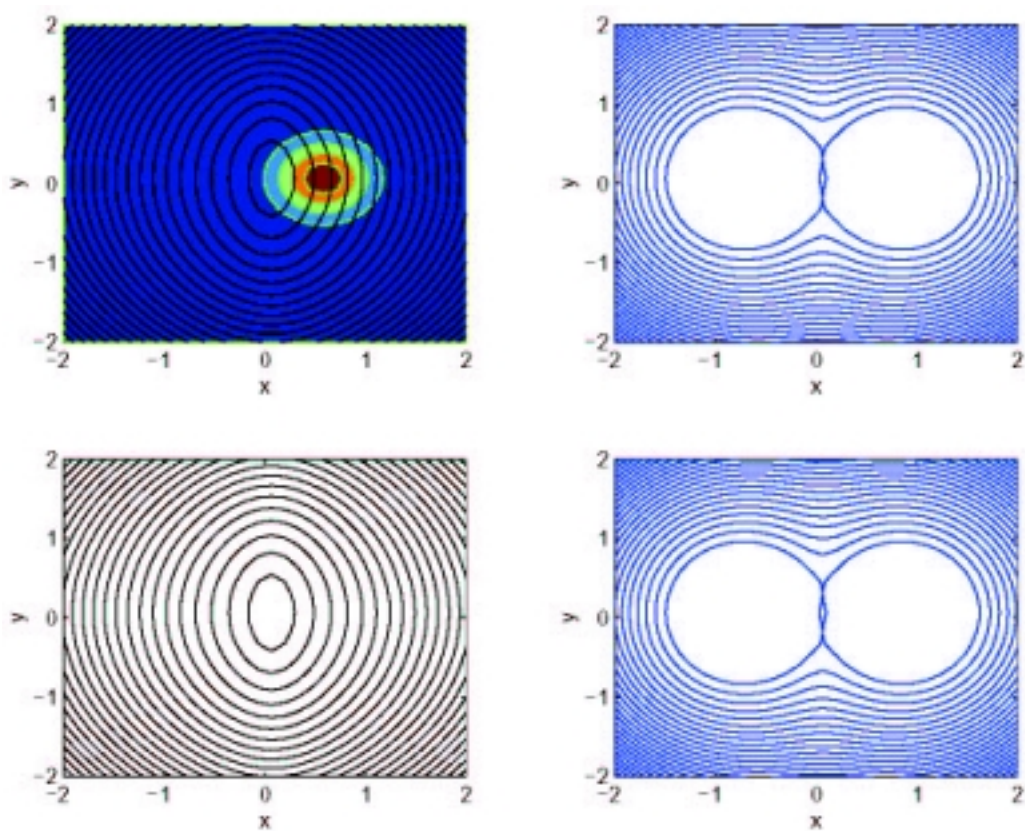


Fig. 9a. The initial diabatic density matrix represented on the adiabatic surface.

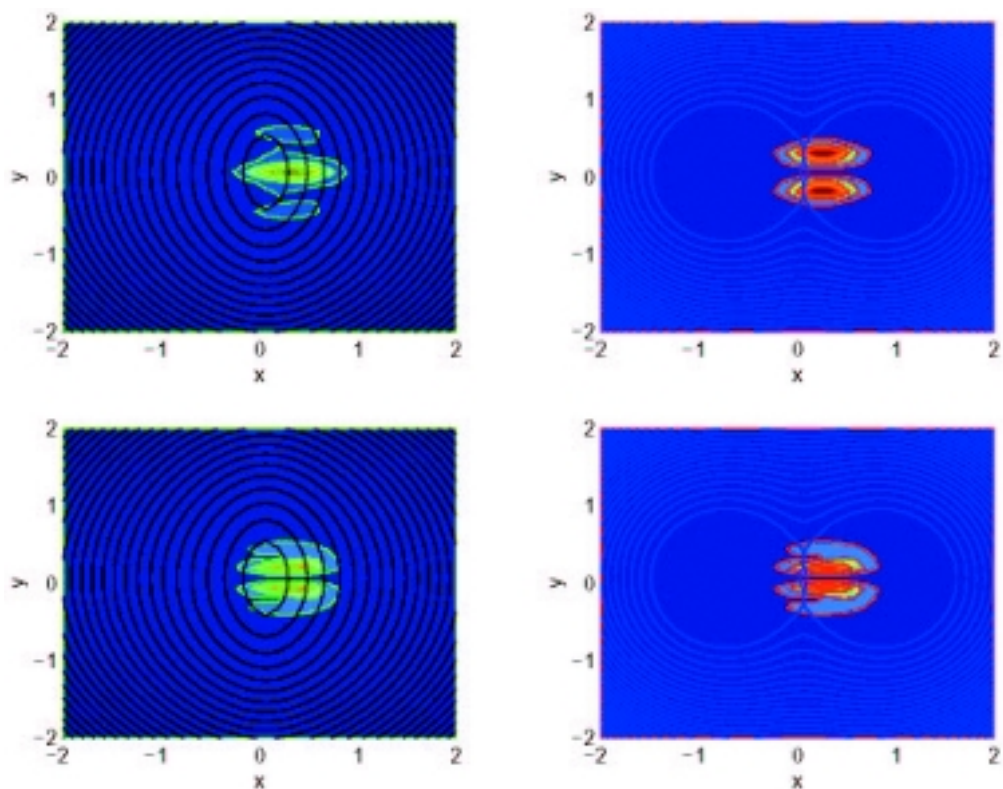


Fig. 9b. The diabatic density matrix represented on the adiabatic surface after 150 fs (clockwise from upper left $L > L$, $R > R$, $R > L$, and $L > R$, where R —right, L —left) for zero perpendicular kinetic energy.

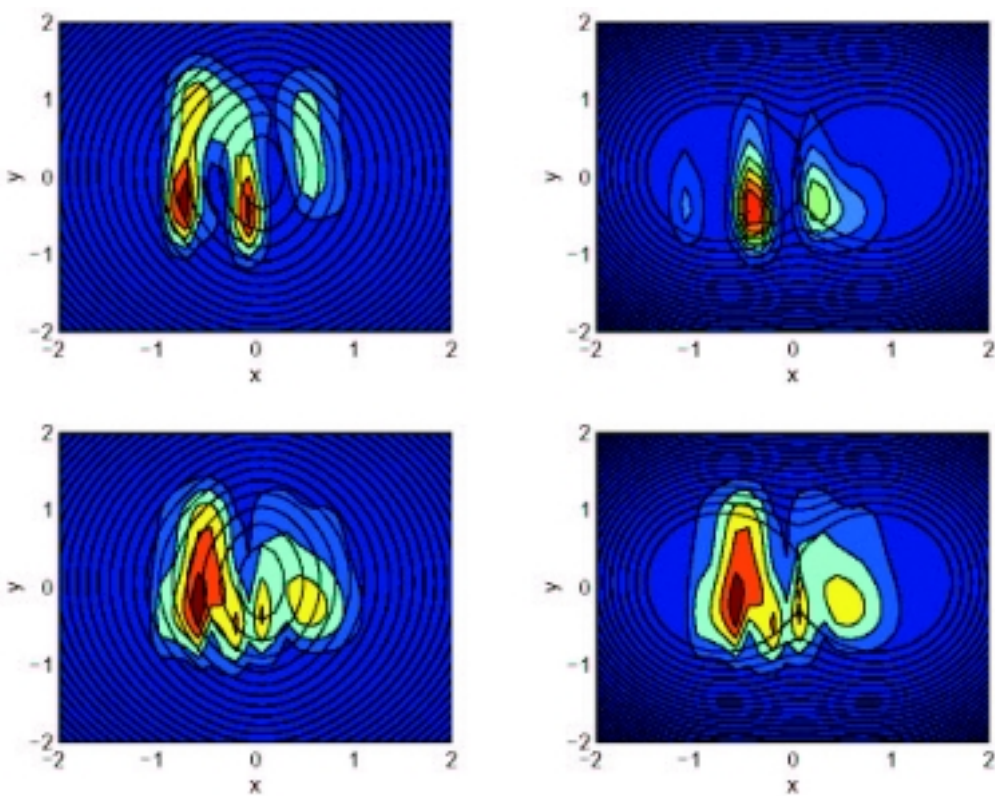


Fig. 9c. Same as 9b for 0.2 eV perpendicular kinetic energy.

after the Franck–Condon excitation. It shows the pure wave packet, which is just the localized ground-state eigenfunction, promoted to the $|L\rangle$ state. At this time, ρ_{RR} , ρ_{LR} , and ρ_{RL} vanish identically. Note that the upper adiabatic state has a single minimum and the ground adiabatic state has a symmetric double minimum, as follows from eqs 4a and 4b.

After a time of 150 fs has evolved, Fig. 9b and 9c show the density matrix elements. These plots show the populations (upper row) and the coherences (lower row). In Fig. 9b, the initial y momentum on the excited surface vanishes. The ρ_{ii} and ρ_{ij} are symmetric around $y = 0$. Note also that very little of ρ_{RR} is found at the origin, consistent with the bleach recovery data of Fig. 8. Figure 9c differs from Fig. 9b only because the momentum along y is finite, starting from an initial value of 0.2 eV for the kinetic energy. Note that the populations and (especially) the coherences ρ_{RL} and ρ_{LR} are much more delocalized. The partial bleach recovery for $1/T_2 > 10^{-4}$ eV reflects the role of $1/T_2$ in mixing the trajectories along the x -coordinate. This same effect is promoted by an initial momentum along y .

IV. REMARKS

The dynamics of excited systems undergoing motion on conical intersections are complex. One expects that dephasing and relaxation terms should reduce the importance of long-lived coherences and phase memory. Since conical intersection dynamics involve both pure angle variables circling the conical apex, and vibration/relaxation motion towards and through the conical tip apex, as well as subsequent vibrational relaxation on the ground surface, the dissipative effects might be expected to modify the dynamics significantly. This has been demonstrated previously, using both all-mode analysis²⁰ and relaxation schemes.^{22–31}

Here we employ a semi group-based method for describing electronic relaxation and dephasing, as well as vibrational relaxation. The simulations for the system density matrix are carried out for true conical potentials, as well as for symmetrized and constant forms for the mixing.

We indeed find substantial sensitivity to the electronic dephasing and vibrational relaxation magnitudes, as well as to the form of the mixing potential. Due to the antisymmetric form of the conical interaction in the y coordinate, the recovery of the initial-state bleach shows marked sensitivities both to the initial momentum along the y coordinate and to the value of the electronic dephasing. For very small electronic dephasing strength $1/T_2$ or for zero initial y momentum, the recovery is very inefficient on the conical surface, but it is far larger if the symmetrized or constant mixings are assumed.

Note the very small absolute values of the computed bleach recovery in Figs. 7 and 8 occur because we have not permitted either vibrational dephasing or vibrational (bath) relaxation in the y node. Therefore (see Fig. 9c), the population on the ground adiabatic surface remains vibrationally excited on the timescale of Figs. 7 and 8.

Accurate bleach recovery calculations require appropriate bath interactions and projection onto the appropriate spectroscopic ground level.

The physics underlying these marked relaxation and initial condition effects is not yet clear, though Teller pointed out long ago¹¹ that symmetry effects will be dominant at conical intersections. Since such conicals have been demonstrated to be very important for molecules from O_3 to *trans*-stilbene, and since environmental effects would always be anticipated to modify the Hamiltonian evolution, understanding the interplay between Hamiltonian and relaxation dynamics is clearly of significance in various fields of photochemistry, optical excitations, and general molecular transformations. This paper is an initial attempt to characterize some aspects of that relaxation behavior.

Acknowledgments. We are grateful to the BSF and to the Chemistry Division of the NSF for support of this work. This paper is dedicated, with love and respect, to JJ, pioneering and visionary scientist, teacher, statesman, and friend.

REFERENCES AND NOTES

- (1) For an approach that is specifically not based on the Born–Oppenheimer separation, cf. Ohn, Y.; Deumens, E. *Adv. Chem. Phys.* **2002**, *124*, 323.
- (2) Born, M.; Oppenheimer, J.R. *Ann. Phys.* **1927**, *87*, 457. Tinkham, M. *Group Theory and Quantum Mechanics*; McGraw-Hill: New York, 1964.
- (3) Nitzan, A.; Jortner, J. *J. Chem. Phys.* **1972**, *56*, 5200.
- (4) Jortner, J. *J. Chem. Phys.* **1976**, *64*, 4860.
- (5) Jortner, J.; Bixon, M. *Adv. Chem. Phys.* **1999**, *106*, 35.
- (6) Zener, C. *Proc. R. Soc. London, Ser. A* **1932**, *137*, 696.
- (7) Nakamura, H. *Nonadiabatic Transition* (World: River Edge, NJ, 2002); Baer, M. *Adv. Chem. Phys.* **2002**, *124*, 39.
- (8) Marcus, R.A. *Annu. Rev. Phys. Chem.* **1964**, *15*, 155.
- (9) Hush, N.S. *Trans. Faraday Soc.* **1961**, *57*, 557.
- (10) Marcus, R.A. *J. Chem. Phys.* **1956**, *24*, 966. Barbara, P. Meyer, T.J.; Ratner, M.A. *J. Phys. Chem.* **1996**, *100*, 13148.
- (11) Teller, E. *J. Phys. Chem.* **1937**, *41*, 109.
- (12) Carrington, T. *Faraday Discuss. Chem. Soc.* **1972**, *53*, 27.
- (13) Davidson, E.R. *J. Am. Chem. Soc.* **1977**, *99*, 397.
- (14) Domcke, W.; Koppel, H.; Cederbaum, L.S. *Mol. Phys.* **1981**, *43*, 851.
- (15) Mead, C.A.; Truhlar, D.G. *J. Chem. Phys.* **1979**, *70*, 2284.

- (16) (a) Klessinger, M.; Michl, J. *Excited States and Photochemistry*; VCH: New York, 1993. (b) Michl, J.; Bonacic-Koutecky, V. *Electronic Aspects of Organic Photochemistry*; Interscience: New York, 1990. (c) Quenneville, J.; Martinez, T. *J. Phys. Chem. A* **2003**, *107*, 829.
- (17) Yarkony, D.R. *Int. Rev. Phys. Chem.* **1992**, *11*, 195.
- (18) Yarkony, D.R. *J. Phys. Chem.* **2001**, *A 105*, 6277.
- (19) Köppel, H. *Chem. Phys. Lett.* **1993**, *205*, 361.
- (20) Cattarius, C.; Worth, G.A.; Meyer, H.-D.; Cederbaum, L.S. *J. Chem. Phys.* **2001**, *115*, 2088. Worth, G.A.; Meyer, H.-D.; Cederbaum, L.S. *J. Chem. Phys.* **1998**, *109*, 3518.
- (21) Klessinger, M. *Angew. Chem.* **1995**, *107*, 597.
- (22) Bernardi, F.; Olivucci, M.; Robb, M. *Chem. Soc. Rev.* **1996**, *25*, 321.
- (23) Krempel, S.; Winterstetter, M.; Pl'hn, H.; Domcke, W. *J. Chem. Phys.* **1995**, *100*, 926.
- (24) Worth, G.A.; Meyer, H.-D.; Cederbaum, L.S. *J. Chem. Phys.* **1999**, *109*, 936.
- (25) Manthe, U.; Köppel, H.; Cederbaum, L.S. *J. Chem. Phys.* **1991**, *95*, 1708.
- (26) Cederbaum, L.S.; Domcke, W.; Köppel, H.; von Niessen, W. *Chem. Phys.* **1977**, *26*, 169.
- (27) Mahapatra, S.; Worth, G.A.; Meyer, H.-D.; Cederbaum, L.S.; Köppel, H. *J. Phys. Chem.* **2001**, *A 105*, 5567.
- (28) Gerdts, T.; Manthe, U. *J. Chem. Phys.* **1997**, *106*, 3017.
- (29) Wolfseider, B.; Domcke, W. *Chem. Phys. Lett.* **1995**, *235*, 370.
- (30) Kuhl, A.; Domcke, W. *J. Chem. Phys.* **2002**, *116*, 263.
- (31) Kuhl, A.; Domcke, W. *Chem. Phys.* **2000**, *259*, 227.
- (32) Lindblad, G. *Commun. Math. Phys.* **2001**, *114*, 2601.
- (33) Rice, S.A.; Kosloff, R. *J. Chem. Phys.* **1980**, *72*, 4591.
- (34) Kohen, D.; Marston, C.C.; Tannor, D. *J. Chem. Phys.* **1997**, *107*, 52361.
- (35) Kosloff, R.; Ratner, M.A. *J. Chem. Phys.* **1982**, *77*, 2841.
- (36) Bartana, A.; Kosloff, R.; Tannor, D.J. *J. Chem. Phys.* **1997**, *106*, 1435–1448.
- (37) Kosloff, R.; Ratner, M.A.; Davis, W.B. *J. Chem. Phys.* **1997**, *106*, 7036–7043.
- (38) Ashkenazi, G.; Kosloff, R.; Ratner, M.A. *J. Am. Chem. Soc.* **1999**, *121*, 3386–3395.
- (39) Koch, C.P.; Kluner, T.; Kosloff, R. *J. Chem. Phys.* **2002**, *116*, 7983–7996.
- (40) Kosloff, R. *J. Phys. Chem.* **1988**, *92*, 2087.
- (41) Saalfrank, P.; Kosloff, R. *J. Chem. Phys.* **1996**, *105*, 2441.
- (42) Kosloff R.; Ratner, M.A. *J. Phys. Chem. B* **2002**, *106*, 8479.
- (43) Cederbaum, L.S.; Friedman, R.S.; Ryaboy, V.M.; Moiseyev, N. *Phys. Rev. Lett.* **2003**, *90*, 013001.
- (44) Saalfrank, P.; Baer, R.; Kosloff, R. *Chem. Phys. Lett.* **1994**, *230*, 463.
- (45) Katz, G.; Zeiri, Y.; Kosloff, R. *Chem. Phys. Lett.* **2002**, *358*, 284.
- (46) Kleinekathofer, U.; Kondov, I.; Schreiber, M. *Chem. Phys.* **2001**, *268*, 121.
- (47) Egorova, D.; Kuhl, A.; Domcke, W. *Chem. Phys.* **2001**, *268*, 105.
- (48) The referee has very helpfully pointed out that since the form of eq 9 derives from assuming that the bath couples to (exchanges quanta with) the diabatic vibration, substantial issues arise, especially in conical structures where the adiabatic vibrational coordinates can have a very different energy spectrum from the diabatic. There is a challenging issue here, that involves the partitioning of system and bath, and the specification of which system modes are appropriately described (using the Lindblad approach) as bilinearly coupled to bath oscillators. This problem is addressed in refs 46 and 47 and an intriguing approach using a super symmetry operator is presented in ref 49. For our purposes here, the diabatic choice seems appropriate for relaxation (eq 9), although this might be more problematic for vibrational dephasing, which we do not address. Egorova et al.⁴⁷ refer to the assumption that the diabatic coordinates couple to the bath as the diabatic damping approximation, and their investigations suggest that it is valid over a broad set of conditions.
- (49) Nest, M.; Saalfrank, P. *Chem. Phys.* **2001**, *268*, 65.
- (50) The referee has pointed out that the form of eq 6 is unphysical, because it has no Taylor expansion around $y = 0$. Similarly, eq 7 has no Taylor expansion around $y = 1/a$. These forms are adopted here only to examine how different potential symmetries affect the dynamic evolution of the excited-state packet. The true conical form of eq 5 is the one whose behavior we wish to understand; to that end, we also examine behaviors with the other forms (6–8).